

# An Aluminophosphate Molecular Sieve with 36 Crystallographically Distinct Tetrahedral Sites\*\*

Jun Kyu Lee, Alessandro Turrina, Liangkui Zhu, Seungwan Seo, Daliang Zhang, Paul A. Cox, Paul A. Wright, Shilun Qiu, and Suk Bong Hong\*

Dedicated to Professor In-Sik Nam

**Abstract:** The structure of the new medium-pore aluminophosphate molecular sieve PST-6 is determined by the combined use of rotation electron diffraction tomography, synchrotron X-ray powder diffraction, and computer modeling. PST-6 was prepared by calcination of another new aluminophosphate material with an unknown structure synthesized using diethylamine as a structure-directing agent, which is thought to contain bridging hydroxy groups. PST-6 has 36 crystallographically distinct tetrahedral sites in the asymmetric unit and is thus crystallographically the most complex zeolitic structure ever solved.

There is a constant drive to search for new zeolitic materials because of their impact on innovation in catalysis and separation, and also on the evolution of emerging technologies.<sup>[1]</sup> Consequently, the number of zeolite framework type codes (FTCs) assigned by the Structure Commission of the International Zeolite Association (SC-IZA) continues to grow steadily. It was in the early 1980s when researchers at Union Carbide (now UOP) announced the synthesis of a family of aluminophosphate molecular sieves, abbreviated

as  $\text{AlPO}_4\text{-n}$ , where in most cases n refers to a distinct framework type.<sup>[2,3]</sup> At present, the SC-IZA recognizes 218 FTCs, 44 of which are known to occur as  $\text{AlPO}_4$ -based frameworks.<sup>[4]</sup> Although  $\text{AlPO}_4$  based molecular sieves display considerable structural diversity, their maximum structural complexity is much lower than that of silica-based materials. This is mainly because of the crystal-chemical requirement that  $\text{AlO}_4$  and  $\text{PO}_4$  tetrahedra must alternate, so that only even-numbered rings are present in the framework, and not odd-numbered rings like the 5-rings found in many of the most complex zeolites. The most complex zeolite structure solved is the large-pore zeolite ITQ-39, the polymorphs A and B of which, with 28 crystallographically-distinct tetrahedral sites (T-sites), are the two most complex structures known to date.<sup>[5]</sup> By contrast, with 12 distinct T-sites, DAF-1 (DFO) is the most complex among the  $\text{AlPO}_4$ -based molecular sieves.<sup>[6]</sup>

Here, we report that an  $\text{AlPO}_4$  molecular sieve denoted PST-6 (POSTECH number 6) has 36 crystallographically distinct (Al, P) atoms of equal multiplicity and 72 such O atoms in the asymmetric unit. Its structure has been determined and refined by a combination of electron crystallography, X-ray powder diffraction, and computer simulation.<sup>[7,8]</sup> Leaving aside SSZ-57 (\*SFV), a modulated zeolite whose “idealized” unit cell possesses 99 symmetrically independent T-sites,<sup>[9]</sup> PST-6 is crystallographically more complex than any zeolitic material known. It is also the first medium-pore material which contains a one-dimensional (1D) pore system consisting of parallel 10- and 8-ring channels.

PST-6 was obtained by the calcination at 550 °C of another new  $\text{AlPO}_4$  phase with a bulk Al/P ratio of unity denoted PST-5. PST-5, whose structure remains unknown, was synthesized using diethylamine (DEA), a common organic structure-directing agent yielding many zeolites and  $\text{AlPO}_4$ -based molecular sieves with different framework topologies.<sup>[10,11]</sup> Its synthesis was found to be highly sensitive to the concentration of DEA in the starting synthesis gel, as well as to the type of the Al source employed (see Table S1 in the Supporting Information).

PST-5 crystallizes as thin plates with a very low aspect ratio ( $\leq 0.05$ ; Figure S1).  $^{27}\text{Al}$  and  $^{31}\text{P}$  MAS NMR spectroscopies indicate that its structure is not fully tetrahedrally connected (Figure S2). Since a wide variety of 2D layered  $\text{AlPO}_4$  networks with Al/P ratios of  $\leq 1.0$  has long been recognized,<sup>[12]</sup> we attempted to swell PST-5 according to the same procedure as that used for the preparation of ITQ-2<sup>[13]</sup> but without success, suggesting it is not a layered material.

[\*] J. K. Lee, S. Seo, Prof. S. B. Hong  
Center for Ordered Nanoporous Materials Synthesis  
School of Environmental Science and Engineering and  
Department of Chemical Engineering, POSTECH  
Pohang 790-784 (Korea)  
E-mail: sbhong@postech.ac.kr

A. Turrina, Prof. P. A. Wright  
School of Chemistry, University of St. Andrews, Purdie Building  
St. Andrews KY16 9ST (UK)

L. Zhu, Dr. D. Zhang, Prof. S. Qiu  
State Key Laboratory of Inorganic Synthesis & Preparative  
Chemistry  
Jilin University, Changchun 130012 (P. R. China)

Dr. P. A. Cox  
School of Pharmacy and Biomedical Sciences, University of Portsmouth  
Portsmouth PO1 2DT (UK)

[\*\*] This work was supported by the NCRI (grant number 2012R1A3A-2048833) and BK 21-plus programs through the National Research Foundation of Korea, POSCO, and the National Natural Science Foundation of China (grant numbers 91022030, 21261130584, 21201076, and 11227403). A.T. acknowledges Johnson Matthey (UK), for financial support. We thank PAL, Korea, and Diamond Light Source (DLS) (UK), for synchrotron diffraction beam time, and Prof. C. C. Tang (DLS) for assistance.

Supporting information for this article is available on the WWW under <http://dx.doi.org/10.1002/anie.201402495>.

Calcination of PST-5 gives PST-6 crystals with the same morphology: the individual plates remain as single crystals, implying that the transformation is topotactic (Figures S1 and S3). Thermogravimetric and differential thermal analyses reveal that PST-5 gives a large endothermic weight loss (ca. 12 wt %) at temperatures up to 350 °C (Figure S4), similar to that observed for  $\text{AlPO}_4\cdot 21$  (AWO), one of the  $\text{AlPO}_4$  molecular sieves prepared using DEA in this work. The DEA molecules in both PST-5 and  $\text{AlPO}_4\cdot 21$  were found to be intact and protonated (Figures S5 and S6). Like the  $^1\text{H}$  MAS NMR spectrum of  $\text{AlPO}_4\cdot 21$ , the spectrum of PST-5 shows a strong  $^1\text{H}$  resonance at 5.0 ppm (Figure S7) that cannot be attributed simply to the protons of occluded water molecules. Drawing an analogy with  $\text{AlPO}_4\cdot 21$  containing 3- and 5-rings in which two adjacent trigonal-bipyramidal Al atoms share a hydroxyl group,<sup>[14]</sup> it is likely that PST-5 may also contain such bridging hydroxyls. Unfortunately, our attempts to index the high resolution synchrotron powder X-ray diffraction (PXRD) pattern of PST-5 have so far been unsuccessful.

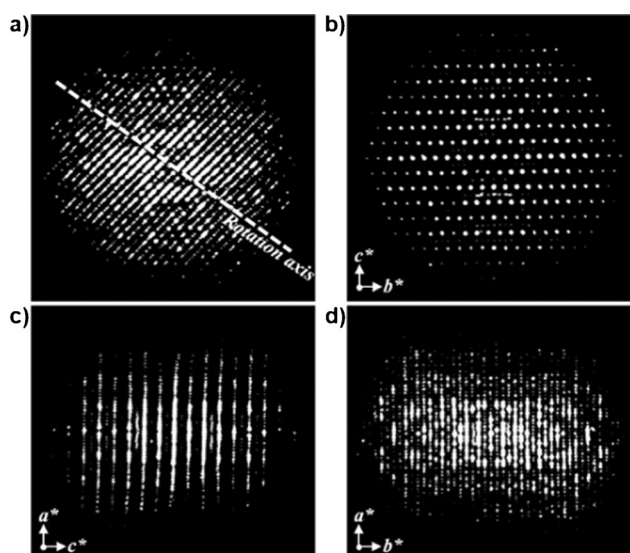
For the PST-6 obtained by calcination of PST-5, initial attempts to index its XRD pattern were unsuccessful. Also, we were unable to get good high-resolution transmission electron microscopy images due to the poor stability of PST-6 in the incident 200 kV electron beam. However, we were able to collect 3D electron diffraction data using the rotation electron diffraction (RED) tomography technique that has been used to solve the structures of nanosized, highly complex zeolites such as ITQ-39 and ITQ-51.<sup>[5,15]</sup> In total, 1178 electron diffraction frames were collected automatically at intervals of 0.1° rotation from one single PST-6 crystal, covering 117° (65%; –63 to 54°) of the 180° required for obtaining complete 3D data.

Figure 1 shows the 3D reciprocal lattice of PST-6 reconstructed using the software RED.<sup>[16]</sup> The selected-area

electron diffraction (SAED) patterns of  $\text{AlPO}_4$  phase taken along [100], [010], and [001] zone axes can be found in Figure S8. It was possible to derive approximate unit cell parameters ( $a = 39.136 \text{ \AA}$ ,  $b = 22.547 \text{ \AA}$ ,  $c = 8.529 \text{ \AA}$ ,  $\alpha = 90.60^\circ$ ,  $\beta = 89.45^\circ$ ,  $\gamma = 89.88^\circ$ ; Figures S8 and S9). As shown in Figure 1, however, there are additional reflections which led us to consider a  $c$ -axis doubling. Because no clear evidence for these reflections is observed in the synchrotron PXRD data, on the other hand, we could not claim that their appearance is irrelevant to the dynamical effects of electron diffraction. Hence, we attempted to combine RED and PXRD data in a structure determination procedure. The unit cell parameters obtained from the electron diffraction results were used to assign indices to the peaks in the synchrotron PXRD pattern of hydrated PST-6. Although some X-ray peaks (later found to be from impurities) were not well matched, the unit cell parameters were refined to be  $a = 39.6500 \text{ \AA}$ ,  $b = 22.2547 \text{ \AA}$ ,  $c = 8.3450 \text{ \AA}$  in orthorhombic ( $Pba2$ ) symmetry, and a model for the  $\text{AlPO}_4$  structure was achieved using the direct methods program EXPO2009.<sup>[17]</sup> After being minimized in energy using the program GULP,<sup>[18]</sup> adopting the interatomic potentials derived by Gale and Henson,<sup>[19]</sup> this model was used as a starting point for the Rietveld refinement of the structures of hydrated and dehydrated PST-6.

For hydrated PST-6, the positions of adsorbed water were determined from the difference Fourier analysis and subsequently refined. Final  $R_{\text{wp}}$  and  $R_p$  values of 10.3 and 7.5 % were achieved, respectively. The final Rietveld plot in Figure S10 provides a reasonable match between the observed and simulated PXRD patterns. The final atomic positions for hydrated PST-6 with a refined unit cell composition  $[(\text{H}_2\text{O})_{16.0}] [\text{Al}_{72}\text{P}_{72}\text{O}_{288}]$  are listed in Table S2, and its final refined structure with  $a = 39.5874(10) \text{ \AA}$ ,  $b = 22.2714(7) \text{ \AA}$ ,  $c = 8.32807(15) \text{ \AA}$  ( $Pba2$ ), is shown in Figure S11. The average Al–O and P–O bond lengths (1.72(2) and 1.53(2) Å, respectively) and average O–Al–O and O–P–O angles (109(3)°) were restrained to be those expected for zeotypic  $\text{AlPO}_4$  materials (Table S3). Attempts to locate the water molecules coordinated to Al atoms, as suggested by the  $^{27}\text{Al}$  MAS NMR results that show the existence of a small amount of penta- and hexa-coordinated Al (Figure S2), were unsuccessful. It is likely that the water molecules are distributed in a disordered way over the framework of PST-6.

The structure of dehydrated PST-6, the  $^{27}\text{Al}$  and  $^{31}\text{P}$  MAS NMR spectra of which indicate a fully tetrahedrally coordinated framework, was refined against synchrotron PXRD data on a sample heated at 300 °C under vacuum (Figure 2). A close fit to the data was achieved and details of the structure refinement can be found in Tables S4–S6. The unit cell changed to  $a = 38.2793(3) \text{ \AA}$ ,  $b = 22.4638(2) \text{ \AA}$ , and  $c = 8.36197(6) \text{ \AA}$  ( $Pba2$ ) upon loss of water, showing a significant decrease in the  $a$ -axis and a smaller increase in the  $b$ - and  $c$ -axes (Figure S12). This can be attributed to the framework relaxation as the water molecules coordinated to some framework Al atoms were removed. To investigate the observation of an apparent  $c$ -axis doubling during the RED experiments, energy minimization of a model with a doubled



**Figure 1.** a) 3D reconstructed reciprocal space viewed perpendicular to the rotation axis of data acquisition. b–d) Projections of the 3D reconstructed reciprocal space viewed along the  $a^*$ -,  $b^*$ -, and  $c^*$ -axes, respectively.

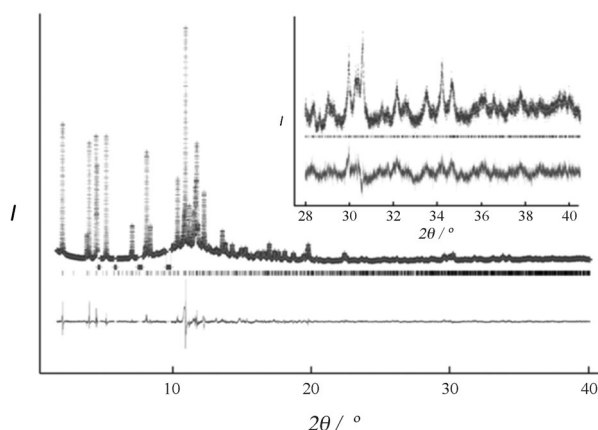


**Figure 2.** Rietveld plot for dehydrated PST-6: observed data (crosses), calculated fit (solid line), difference plot (lower trace). Tick marks show the positions of allowed reflections; minor impurity peaks are excluded (synchrotron,  $\lambda = 0.825621$  Å).

cell in the *c*-axis was attempted, but no evidence for a superstructure was found.

PST-6 contains a 1D pore system consisting of two parallel, elliptical 10-ring ( $4.2 \times 6.6$  Å) and 8-ring ( $2.3 \times 6.0$  Å) channels running along the *c*-axis which are separated by framework walls perpendicular to the *a*- and *b*-axes (Figure 3 and Figure S11). This material is characterized by

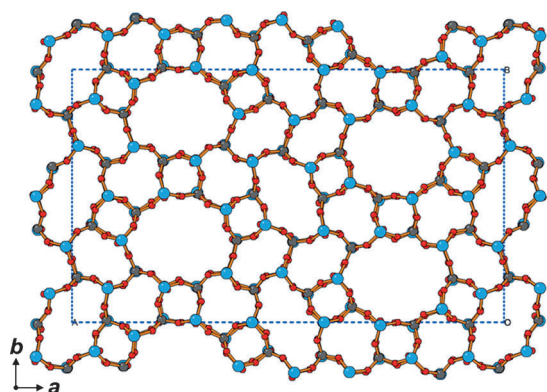


**Figure 3.** Framework structure of dehydrated PST-6 with two parallel, highly elliptical 10- and 8-ring channels running along the *c*-axis. Al, light blue; P, dark gray; O, red.

a framework density (defined as the number of T-atoms per  $1000$  Å<sup>3</sup>) of 19.6 which is quite high when compared with other 10-ring pore materials.<sup>[4]</sup> We also note that the *a*-axis is perpendicular to the short dimension of the thin crystals and, structurally at least, the framework is composed of thick sheets parallel to the *bc* plane, related by a center of symmetry across double crankshaft chains (with 4-ring projections), typical of AlPO<sub>4</sub> molecular sieves. In fact, the Ar sorption experiments indicate that PST-6 possesses a low micropore volume of  $0.04$  cm<sup>3</sup> g<sup>-1</sup> (Figure S13). Considering its unique 1D pore structure, however, PST-6 could find applications in the selective separation of small gases like H<sub>2</sub> or CO<sub>2</sub> based on the concept of molecular traffic control.<sup>[20]</sup>

With 36 crystallographically distinct (Al, P) atoms of equal multiplicity, the framework structure of this new AlPO<sub>4</sub> molecular sieve is crystallographically more complex than any of the already known zeolite structures. Considering its maximum topological symmetry, that is, considering Al and P identical, it is also one of the most complex zeolitic structures known, and by far the most complex AlPO<sub>4</sub> molecular sieve. The reason PST-6 has such a large number (18) of topologically distinct T-sites, well beyond those of other compositionally simple AlPO<sub>4</sub> molecular sieves with even-numbered rings, is not yet clear. However, the <sup>27</sup>Al and <sup>31</sup>P MAS NMR spectra of PST-5 (Figure S2), the precursor of PST-6, reveal that its framework contains penta-coordinated Al atoms, as well as tetrahedral Al atoms, and a wide range of tetrahedral P environments, with a range ( $-15.1$ – $32.1$  ppm) of <sup>31</sup>P chemical shifts. This range is comparable to that ( $-13.3$ – $30.3$  ppm) observed for AlPO<sub>4</sub>-21 which has hydroxyl groups bridging between Al atoms.<sup>[21]</sup> Therefore, we think that the PST-5 framework may possess odd-numbered 3- and/or 5-rings in which Al-O-Al linkages may exist. If such is the case, it is less surprising that the precursor PST-5 has a very complex structure, features of which are inherited upon removal of template and bridging hydroxyls during calcination to yield a very complex zeolite structure with tetrahedral Al and P atoms only, that is, PST-6.

In summary, we have synthesized a new medium-pore AlPO<sub>4</sub> molecular sieve denoted PST-6 and solved its structure by combining powder diffraction, electron crystallography, and computer modeling. PST-6 has 36 crystallographically distinct (Al, P) atoms and 72 such O atoms in the asymmetric unit and thus ranks as the most crystallographically complex zeolite structure known to date. It is also the first molecular sieve with a 1D system of two parallel 10- and 8-ring channels. This shows that novel, highly complex zeolite structures that contain even-numbered rings only can arise at a simple AlPO<sub>4</sub> composition.

## Experimental Section

In a typical synthesis of PST-5, 3.84 g of *o*-H<sub>3</sub>PO<sub>4</sub> (85%, Merck) were first dissolved in 5.63 g of H<sub>2</sub>O. This solution was added dropwise to a slurry of 6.95 g of aluminum isopropoxide ( $\geq 98\%$ , Aldrich) in 5.64 g of H<sub>2</sub>O. After being stirred for 1 h, 2.45 g of DEA (99.5%, Aldrich) were added. The final composition of the synthesis mixture was 2.0DEA·1.0Al<sub>2</sub>O<sub>3</sub>·1.0P<sub>2</sub>O<sub>5</sub>·40H<sub>2</sub>O. The synthesis mixture was stirred overnight at room temperature, charged into Teflon-lined 23 mL autoclaves, and heated at 200 °C for 5 days. PST-6 was prepared by calcination of PST-5 under flowing air at 550 °C for 8 h.

Synchrotron PXRD data for PST-6 in hydrated and dehydrated forms were collected on the 9B beamline of the Pohang Acceleration Laboratory (Pohang, Korea) using monochromated X-rays ( $\lambda = 1.54740$  Å) and on the I11 beamline of the Diamond Light Source (Didcot, UK) using monochromated X-rays ( $\lambda = 0.825621$  Å), respectively. Details of the XRD measurements and Rietveld refinements can be found in Supporting Information.

Received: February 17, 2014

Revised: April 21, 2014

Published online: May 26, 2014

**Keywords:** aluminophosphates · microporous materials · structure elucidation · tetrahedral sites · zeolites

- [1] M. A. Camblor, S. B. Hong in *Porous Materials* (Ed.: D. W. Bruce, D. O'Hare, R. I. Walton), Wiley, Chichester, **2011**, p. 265.
- [2] S. T. Wilson, B. M. Lok, C. A. Messina, T. R. Cannan, E. M. Flanigen, *J. Am. Chem. Soc.* **1982**, *104*, 1146–1147.
- [3] S. T. Wilson, B. M. Lok, E. M. Flanigen, US Pat 4310440, **1982**.
- [4] C. Baerlocher, L. B. McCusker, Database of Zeolite Structures: <http://www.iza-structure.org/databases/>.
- [5] T. Willhammar, J. Sun, W. Wan, P. Oleynikov, D. Zhang, X. D. Zou, M. Moliner, J. Gonzalez, C. Martinez, F. Rey, A. Corma, *Nat. Chem.* **2012**, *4*, 188–194.
- [6] G. Muncaster, G. Sankar, C. R. A. Catlow, J. M. Thomas, R. G. Bell, P. A. Wright, S. Coles, S. J. Teat, W. Clegg, W. Reeve, *Chem. Mater.* **1999**, *11*, 158–163.
- [7] U. Kolb, T. Gorelik, C. Kübel, M. T. Otten, D. Hubert, *Ultra-microscopy* **2007**, *107*, 507–513.
- [8] D. Zhang, P. Oleynikov, S. Hovmöller, X. D. Zou, *Z. Kristallogr.* **2010**, *225*, 94–102.
- [9] C. Baerlocher, T. Weber, L. B. McCusker, L. Palatinus, S. I. Zones, *Science* **2011**, *333*, 1134–1137.
- [10] R. Szostak, *Handbook of Molecular Sieves*, Van Nostrand Reinhold, New York, **1992**.
- [11] Z. Liu, X. Song, J. Li, Y. Li, J. Yu, R. Xu, *Inorg. Chem.* **2012**, *51*, 1969–1974.
- [12] S. Oliver, A. Kuperman, G. A. Ozin, *Angew. Chem.* **1998**, *110*, 48–64; *Angew. Chem. Int. Ed.* **1998**, *37*, 46–62.
- [13] A. Corma, V. Fornes, S. B. Pergher, Th. L. M. Maesen, J. G. Buglass, *Nature* **1998**, *396*, 353–356.
- [14] J. M. Bennett, J. M. Cohen, G. Artioli, J. J. Pluth, J. V. Smith, *Inorg. Chem.* **1985**, *24*, 188–193.
- [15] R. Martínez-Franco, M. Moliner, Y. Yun, J. Sun, W. Wan, X. D. Zou, A. Corma, *Proc. Natl. Acad. Sci. USA* **2013**, *110*, 3749–3754.
- [16] W. Wan, J. Sun, J. Su, S. Hovmöller, X. D. Zou, *J. Appl. Crystallogr.* **2013**, *46*, 1863–1873.
- [17] A. Altomare, M. Camalli, C. Cuocci, C. Giacovazzo, A. Moliterni, R. Rizzi, *J. Appl. Crystallogr.* **2009**, *42*, 1197–1202.
- [18] J. D. Gale, A. L. Rohl, *The General Utility Lattice Program*, *Mol. Simul.* **2003**, *29*, 291–341.
- [19] J. D. Gale, N. J. Henson, *J. Chem. Soc. Faraday Trans.* **1994**, *90*, 3175–3179.
- [20] R. Harish, D. Karevski, G. M. Schütz, *J. Catal.* **2008**, *253*, 191–199.
- [21] R. Jelinek, B. F. Chmelka, Y. Wu, P. J. Grandinetti, A. Pines, P. J. Barrie, J. Klinowski, *J. Am. Chem. Soc.* **1991**, *113*, 4097–4101.